

# Effects of Ammonium Chloride on the Rheological Properties and Sedimentation Behavior of Aqueous Silica Suspensions

J. Jiyou Guo and Jennifer A. Lewis\*

Department of Materials Science and Engineering, University of Illinois, Urbana, Illinois 61801

The influence of ammonium chloride ( $\text{NH}_4\text{Cl}$ ) on the rheological properties and sedimentation behavior of aqueous silica ( $\text{SiO}_2$ ) suspensions of varying solids volume fraction ( $\phi_s$ ) was studied.  $\text{SiO}_2$  suspensions with low  $\text{NH}_4\text{Cl}$  concentration ( $\leq 0.05M$ , pH 5.2) exhibited Newtonian behavior and a constant settling velocity ( $U$ ). The volume fraction dependence was well described by the Richardson–Zaki form,  $U = U_0(1 - \phi_s)^n$ , where  $n = 4.63$  and  $U_0 = 1.0419 \times 10^{-5}$  cm/s. At higher  $\text{NH}_4\text{Cl}$  concentrations (0.07–2.0M, pH 5.2), suspensions exhibited shear thinning and more complicated sedimentation behavior due to their aggregated nature. For all suspensions studied, however, the apparent suspension viscosity, characteristic cluster size, and initial settling velocity were greatest at  $\sim 0.5M$   $\text{NH}_4\text{Cl}$  and exhibited a similar dependence on salt concentration. Above 0.5M  $\text{NH}_4\text{Cl}$ , considerable restabilization was observed. This behavior cannot be explained by traditional DLVO theory.

## I. Introduction

COLLOIDAL processing offers the potential to reliably produce ceramic films and bulk forms by tailoring suspension “structure” through careful control of interparticle potentials. Three types of suspension behavior can be realized through this manipulation: dispersed, weakly flocculated, or strongly flocculated systems.<sup>1–6</sup> It is well known that dispersed systems exhibit improved flow behavior and higher packing densities relative to their flocculated counterparts. However, recent work has shown that weakly flocculated systems prepared with certain additives (e.g., monovalent salts,<sup>4,5</sup> short-chain dispersants,<sup>6</sup> or nonadsorbing polymer species<sup>3</sup>) can be consolidated to packing densities characteristic of those achieved by stable dispersions, despite their increased flow resistance at low shear rates. For example, Lange and co-workers<sup>3,4</sup> have demonstrated that highly salted, aqueous alumina ( $\text{Al}_2\text{O}_3$ ) suspensions can be consolidated to volume fractions approaching 0.60. In such weakly flocculated suspensions, long-range van der Waals attractions between colloidal particles are only partially screened by electrostatic (and possibly hydration) forces at short separation distances such that aggregation occurs in a shallow secondary minima.<sup>1,2</sup> These observations suggest that DLVO theory alone is not sufficient to predict colloidal stability at elevated salt concentrations.

Much attention has been given to the rheological and sedimentation behavior of dispersed systems. One of the most studied model systems, and the simplest, is that of monodisperse hard spheres. An understanding of their suspension rheology<sup>7–9</sup> and sedimentation behavior<sup>10</sup> has been firmly established, and serves as a basis for understanding the more complicated behavior

exhibited by other systems. Unfortunately, the rheological behavior of both stable and flocculated suspensions is often poorly described by hard sphere constitutive responses.<sup>11</sup> In addition, dramatic deviations from hard sphere sedimentation behavior have also been reported for both stable<sup>12</sup> and flocculated suspensions.<sup>13</sup> The observed sedimentation behavior of flocculated systems depends strongly on their solids volume fraction ( $\phi_s$ ). In dilute suspensions, aggregation produces discrete clusters which settle more or less independently. Above some critical volume fraction, known as the gel point ( $\phi_g$ ), the clusters become overcrowded and an inhomogeneous space-filling network (or gel) forms, which may or may not sediment depending on its strength.<sup>13</sup> Philipse *et al.*<sup>14</sup> have studied colloidal filtration of relatively dilute, aggregated silica suspensions and shown that simultaneous aggregate sedimentation leads to deviations from the known linear relationship between compact thickness and the square root of the filtration time as well as a decrease in process time. Carpineti *et al.*<sup>15</sup> have studied fast, salt-induced colloidal aggregation phenomena, and shown that growth from dilute systems ceases because of sedimentation when clusters reach some maximum size. More recently, Allain *et al.*<sup>16</sup> have studied the simultaneous aggregation and sedimentation in colloidal suspensions and have developed a model for relating the settling dynamics of gelled networks to their specific spatial structure. Their work is useful in understanding the various transitions from settling of isolated clusters at  $\phi_s < \phi_g$ , to collective settling of a gel network at  $\phi_s > \phi_g$ , to no settling when  $\phi_s$  approaches an upper critical limit (i.e., when the gel network formed can support itself).

The aim of our work is to study the effects of  $\text{NH}_4\text{Cl}$  concentration on the rheological and sedimentation behavior of aqueous silica suspensions of varying solids volume fraction. For the first time, we show that colloidal suspensions exhibit a maximum instability at a finite  $\text{NH}_4\text{Cl}$  concentration, as demonstrated by their flow properties under both shear and gravitational forces. The origin of this remarkable behavior is not well understood, but likely stems from how such species alter the various interparticle forces (i.e., van der Waals, electrostatic, and, possibly, structural forces) that govern colloidal stability in such systems.

## II. Experimental Procedure

### (I) Materials System and Suspension Preparation

Monodisperse  $\text{SiO}_2$  spheres ( $a = 0.25 \pm 0.05$   $\mu\text{m}$ , GelTECH, Alachua, FL) were used as the colloidal phase. The particle density was 2.25 g/cm<sup>3</sup>, as measured by helium pycnometry (Micrometrics AccuPyc 1330, Norcross, GA). The specific surface area, measured by BET (Micrometrics ASAP 2400, Norcross, GA), was approximately 4.9 m<sup>2</sup>/g, yielding an equivalent spherical diameter of 0.54  $\mu\text{m}$ .

Colloidal suspensions of varying  $\text{SiO}_2$  volume fraction ( $\phi_s = 10^{-4}$ –0.3) were prepared in deionized water and in aqueous solutions with  $\text{NH}_4\text{Cl}$  (Aldrich, Milwaukee, WI) concentrations ranging between 0.01M and 2.0M. Upon addition of the appropriate amount of  $\text{SiO}_2$ , each suspension was stirred for 24 h and intermittently sonicated (550 Sonic Dismembrator, Fisher Scientific, Pittsburgh, PA) every 2 h for a period of 5 min (with a 1 s on/off pulse sequence at 20 kHz). All suspensions were initially

V.A. Hackley—contributing editor

Manuscript No. 189489. Received March 17, 1999; approved August 6, 1999.  
Supported by the National Science Foundation under Grant No. DMR 94-53446.  
\*Member, American Ceramic Society.

adjusted to pH 5.2 ( $\pm 0.1$  pH unit), well above the measured isoelectric point (IEP) of  $\text{SiO}_2$  at pH  $\approx 2$ , using a stock solution of analytical-grade  $\text{NH}_4\text{OH}$  and  $\text{HCl}$ , and then readjusted to this value prior to carrying out the experiments outlined below. Zeta potential analysis (Penkum Lazer Zee Meter 501, Bedford Hills, NY) was performed on dilute, aqueous  $\text{SiO}_2$  suspensions (pH 5.2, 0.01M  $\text{NH}_4\text{Cl}$ ). Under these conditions,  $\text{SiO}_2$  particles were negatively charged with a zeta potential of  $-27$  mV, an average value derived from ten measurements.

## (2) Rheological Measurements

Concentrated suspensions ( $\phi_s = 0.10$ – $0.30$ ) and corresponding aqueous solutions of varying  $\text{NH}_4\text{Cl}$  concentration were characterized using a Bohlin Controlled Stress Rheometer (Bohlin Rheologi CS-10, Cranbury, NJ) fitted with a concentric cylinder (C25) or double concentric cylinder geometry. Rheological measurements were carried out at  $22^\circ\text{C}$ . Most of the measurements were made with the Couette double gap cell (gap widths  $\approx 2$  mm) which allowed measurements up to 30 Pa and down to 0.0035 Pa. When necessary, the C25 cup and bob (bob diameter of 25 mm and gap width of 1.25 mm) was used which extended the measured stress range to 240 Pa. A solvent trap, filled with corresponding solution, was used to minimize evaporation. Measurements could be made over a period of several hours without noticeable changes in transport properties due to drying.

The rheological properties of the colloidal suspensions and corresponding solutions were studied using stress viscometry. The apparent viscosity was measured as a function of shear stress in ascending order. The solutions exhibited Newtonian behavior over the entire shear stress range independent of composition. The rheometer was calibrated with standard silicone oils for all geometries, and viscosity measurements were found to be geometry independent. In addition, the results reported below do not appear to depend significantly on shear history; e.g., analogous results were obtained when measurements were made after pre-shearing suspensions at  $100\text{ s}^{-1}$  to break up the initial aggregates formed or when suspensions were simply slow-rolled in the absence of milling media for 15 min prior to testing.

## (3) Optical Microscopy

Concentrated suspensions ( $\phi_s = 0.1$ ) of varying solution composition were diluted by adding three drops of each suspension to 1 mL of the corresponding solution of varying  $\text{NH}_4\text{Cl}$  concentration. A representative sample of each diluted suspension was placed upon a microscopic slide and then immediately covered with another slide. The edges were sealed with vacuum grease to prevent solvent loss. Three photomicrographs were obtained for each specimen using an optical microscope (Olympus BH-2, Japan). The images were then analyzed using the linear intercept method<sup>17</sup> from which their characteristic floc sizes were determined.

## (4) Sedimentation Measurements

The experimental cells for the sedimentation studies were graduated cylinders (diameter = 2.0 cm, height = 15 cm). As-prepared suspensions of varying colloid volume fraction and salt concentration were transferred to these cylinders to a height of approximately 12.8 cm. Each cell was then capped to minimize solvent loss during the experiment. The origin of the time scale was taken as the suspensions were poured into the cylinder. The top interface separating the supernatant and sediment was then recorded as a function of time. This interface was difficult to distinguish in systems of very low  $\phi_s$ , leading to experimental error in dilute suspensions.

## III. Results

### (1) $\text{NH}_4\text{Cl}$ Effects on Rheological Behavior

A log–log plot of apparent viscosity,  $\eta_{\text{app}}$ , as a function of shear rate is shown in Fig. 1 for  $\text{SiO}_2$  ( $\phi_s = 0.1$ ) suspensions of varying

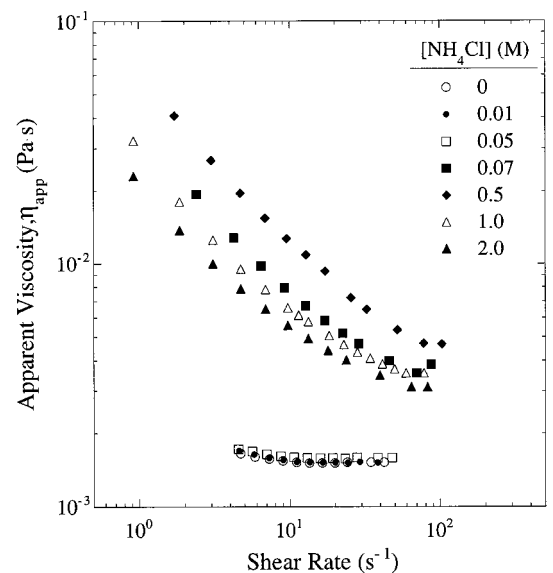


**Fig. 1.** log–log plot of apparent suspension viscosity as a function of shear rate for  $\text{SiO}_2$  suspensions ( $\phi_s = 0.10$ ) of varying solution composition.

$\text{NH}_4\text{Cl}$  concentration in solution, and, hence, stability.  $\text{SiO}_2$  suspensions in deionized water or in aqueous solutions of low  $\text{NH}_4\text{Cl}$  concentration ( $\leq 0.05\text{M}$ ) exhibited Newtonian behavior over the shear stress range studied indicative of a stable or dispersed system. Additional salt ( $\geq 0.07\text{M}$   $\text{NH}_4\text{Cl}$ ) led to higher viscosities and modest shear thinning behavior. The most viscous suspensions were observed when the salt concentration was roughly  $0.5\text{M}$   $\text{NH}_4\text{Cl}$ . Interestingly, further increases in  $\text{NH}_4\text{Cl}$  concentration led to a reduction in suspension viscosity.

The dependence of apparent suspension viscosity (at  $1\text{ s}^{-1}$ ) on salt concentration for  $\text{SiO}_2$  suspensions of varying solids volume fraction ( $\phi_s = 0.1$ – $0.3$ ) is shown in Fig. 2. A dramatic rise in apparent viscosity at low salt concentration was observed in each case, with a maximum viscosity observed at  $0.5\text{M}$   $\text{NH}_4\text{Cl}$  regardless of solids loading. Beyond this critical salt concentration, there

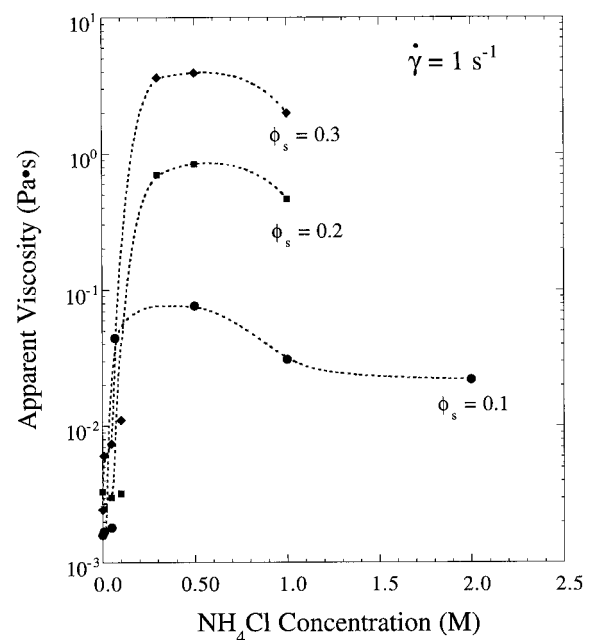


**Fig. 2.** Semilog plot of apparent suspension viscosity as a function of  $\text{NH}_4\text{Cl}$  concentration for varying solids volume  $\text{SiO}_2$  suspension fraction ( $\phi_s = 0.10$ – $0.30$ ).

was a modest decrease in the suspension viscosity indicative of improved stability. Because of specific adsorption interactions between ammonium ions and silica, it is unclear whether this behavior would be expected for all monovalent salt species. However, Lange and co-workers<sup>4</sup> reported similar findings in a related study on aqueous Al<sub>2</sub>O<sub>3</sub> suspensions ( $\phi_s = 0.2$ ), although observed improvements in stability in the high concentration regime ( $\geq 0.5M$  monovalent salt) were neglected in their work.

### (2) NH<sub>4</sub>Cl Effects on Characteristic Floc Structure

Optical micrographs of diluted SiO<sub>2</sub> suspensions of varying solution composition are shown in Fig. 3. The observed features are likely comparable in size to the primary clusters present in each suspension prior to dilution, with “linkages” between clusters disrupted by the dilution process. SiO<sub>2</sub> suspensions in aqueous solutions of low NH<sub>4</sub>Cl concentration ( $\leq 0.05M$ ) were well dispersed and individual particles were observed. Upon increasing NH<sub>4</sub>Cl addition ( $\geq 0.07M$ ), the suspensions became unstable, as demonstrated by an increase in the characteristic floc size ( $D_{\text{floc}}$ ) plotted in Fig. 4. Note, the mean floc size reached a maximum value of roughly 15  $\mu\text{m}$  for suspensions in a 0.5M NH<sub>4</sub>Cl aqueous solution. Interestingly, further NH<sub>4</sub>Cl additions reduced the mean floc size in suspension. Such trends were analogous to the observed rheological behavior with increasing salt concentration. It is not unexpected that suspensions with the largest primary flow units would exhibit a maximum apparent viscosity over the shear rate range probed, as shown in Figs. 1 and 2.

### (3) NH<sub>4</sub>Cl Effects on Sedimentation

Semilog plots of suspension height as a function of settling time are shown in Fig. 5 for SiO<sub>2</sub> suspensions of varying solids loading and solution composition. The data shown in Figs. 5(a) and (b) are representative of those obtained for dispersed (0.01M NH<sub>4</sub>Cl) and weakly flocculated (0.50M NH<sub>4</sub>Cl) systems, respectively. SiO<sub>2</sub> suspensions in aqueous solutions of low NH<sub>4</sub>Cl concentration ( $\leq 0.05M$ ) exhibited a sharp interface between the supernatant and suspension, and required long settling times ( $\sim 10^6$  s) to reach an equilibrium sediment height. The dispersed suspensions exhibited a constant settling velocity, as demonstrated by an excellent linear fit (linear regression coefficient,  $R > 0.99$ ) of the curves shown in the inset of Fig. 5(a). These data were correlated using a Richardson-Zaki form:<sup>18</sup>

$$U = U_0(1 - \phi_s)^n \quad (1)$$

where  $U_0$  is the settling velocity for an isolated sphere determined by Stokes' law:

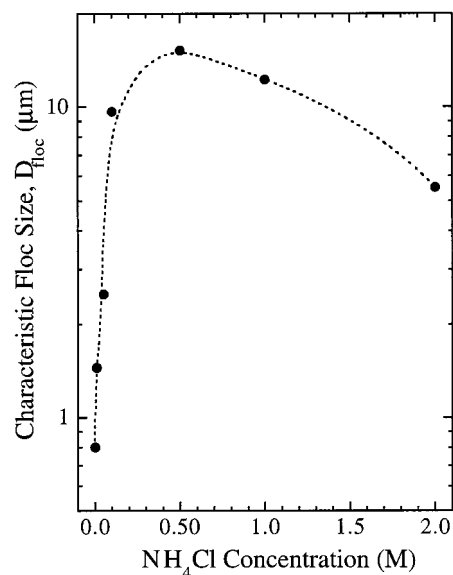


Fig. 4. Semilog plot of characteristic floc size ( $D_{\text{floc}}$ ) as a function of NH<sub>4</sub>Cl concentration of diluted SiO<sub>2</sub> suspensions fraction ( $\phi_s = 0.10$ ).

$$U_0 = \frac{2(\rho_s - \rho)}{9\eta} a^2 g \quad (2)$$

where  $\rho_s$  is the density of the colloidal phase,  $\rho$  is the density of the liquid phase,  $\eta$  is the apparent solution viscosity, and  $g$  is the gravitational constant. A log-log plot of the settling velocity as a function of initial SiO<sub>2</sub> volume fraction is shown in Fig. 6 for suspensions with an NH<sub>4</sub>Cl concentration of 0.01M. The solid line in this plot represents the best power law fit ( $R > 0.99$ ) of the experimental data, where the power law exponent,  $n$ , and the intercept,  $U_0$ , were found to be 4.63 and  $1.0419 \times 10^{-5}$  cm/s, respectively. The exponent is in good agreement with the value of  $n = 4.65$  originally reported by Richardson and Zaki.<sup>18</sup> Using Eq. (2), one calculates a particle radius,  $a$ , of 196 nm for this value of  $U_0$ , which is equivalent to the lower bound of the SiO<sub>2</sub> particle size distribution ( $a = 0.25 \pm 0.05 \mu\text{m}$ ). Hence, not unexpectedly, the settling velocity corresponds to that of the smallest particles in suspension in the dilute limit ( $\phi_s \rightarrow 0$ ).

Upon increasing NH<sub>4</sub>Cl addition, SiO<sub>2</sub> suspensions displayed markedly different sedimentation behavior. At low colloid volume fractions, small aggregates were observed to form and then settle,

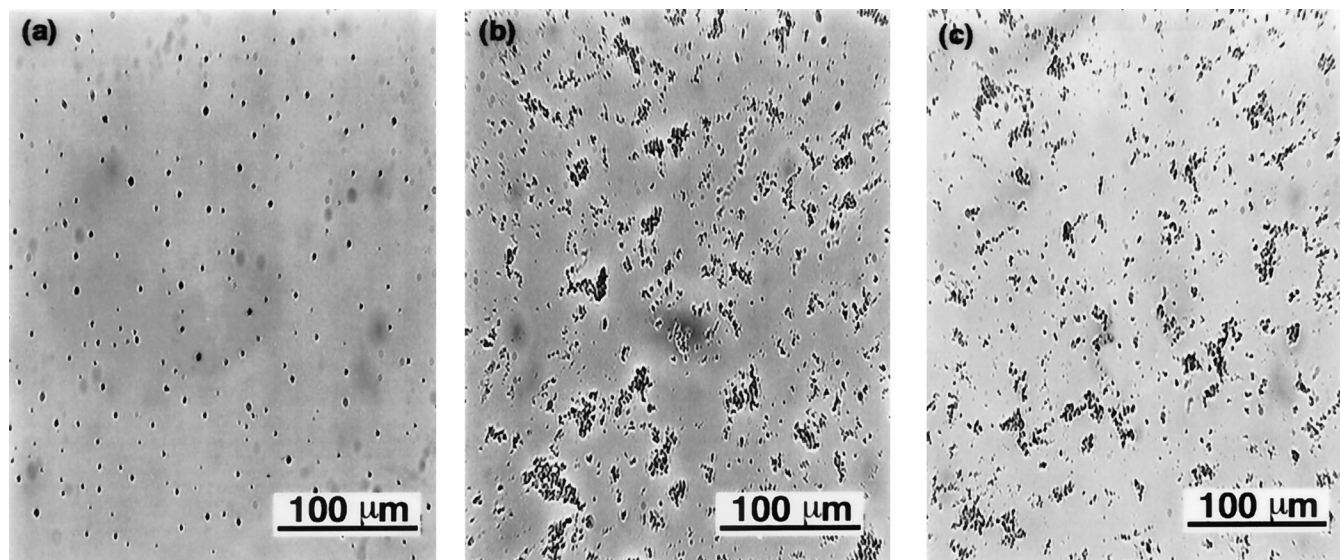
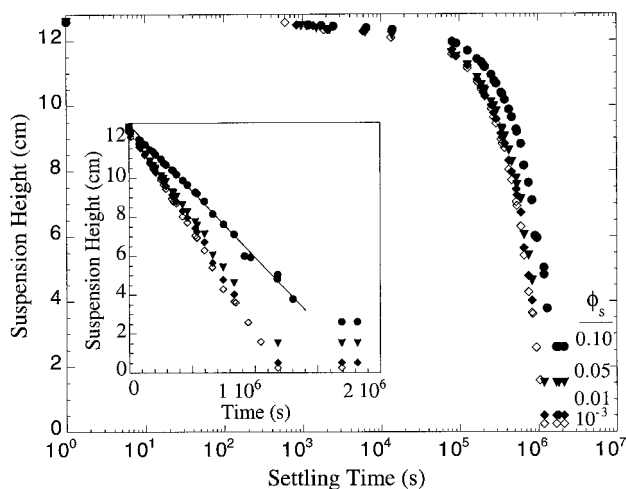
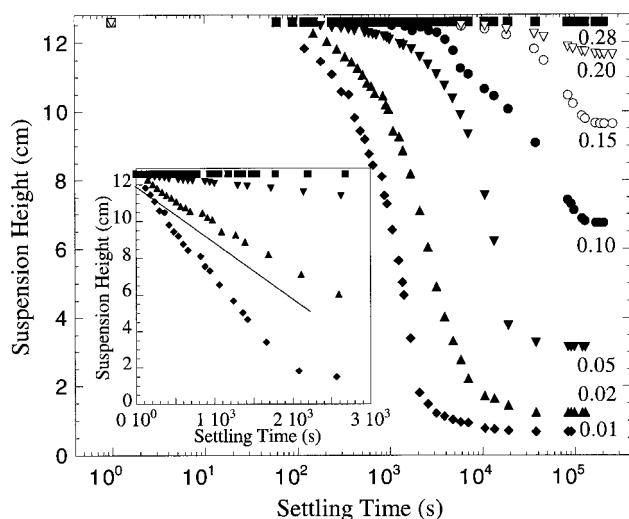


Fig. 3. Optical micrographs of diluted SiO<sub>2</sub> suspensions fraction ( $\phi_s = 0.10$ ) of varying NH<sub>4</sub>Cl concentration: (a) 0.01M, (b) 0.50M, and (c) 2.0M.



(a)



(b)

**Fig. 5.** Semilog plots of suspension height as a function of settling time for  $\text{SiO}_2$  suspensions of varying  $\text{NH}_4\text{Cl}$  concentration and solids volume fraction: (a) 0.01M and (b) 0.50M. (Note: Inset plots depict linear dependence of suspension height on settling time for each system.)

resulting in a hazy interface. This mode, referred to as cluster deposition, occurs when  $\phi_s < \phi_g$ , where  $\phi_g$  is defined as the critical volume fraction for gelation in the presence of gravity-driven mass segregation.<sup>16</sup> In the cluster deposition regime ( $\phi_s < \phi_g \sim 0.05$ ), settling times roughly 2 orders of magnitude lower than those required for sedimentation of dispersed systems of analogous solids loadings were observed, as shown in Fig. 5(b). Moreover, the time required to establish an equilibrium sediment height exhibited a much stronger dependence on  $\phi_s$ . At intermediate  $\text{SiO}_2$  volume fractions, settling of individual aggregates was no longer detected; rather a continuous, gel network formed quickly and then settled collectively. This mode, referred to as collective settling, occurred when  $\phi_g \leq \phi_s < \phi_c$ , where  $\phi_c$  is defined as the upper critical volume fraction.<sup>16</sup> For  $\phi_s > \phi_c$ , settling was not observed during the experimental time frame probed.

The transition between cluster deposition and collective settling can be understood by considering the respective time constants for aggregation ( $\tau_{\text{agg}}$ ) and settling processes ( $\tau_{\text{sed}}$ ) which occur simultaneously during sedimentation of flocculated systems. When  $\tau_{\text{agg}}/\tau_{\text{sed}} \geq 1$ , sedimentation begins prior to gelation and cluster growth may be modified by the settling motion. The gel point is

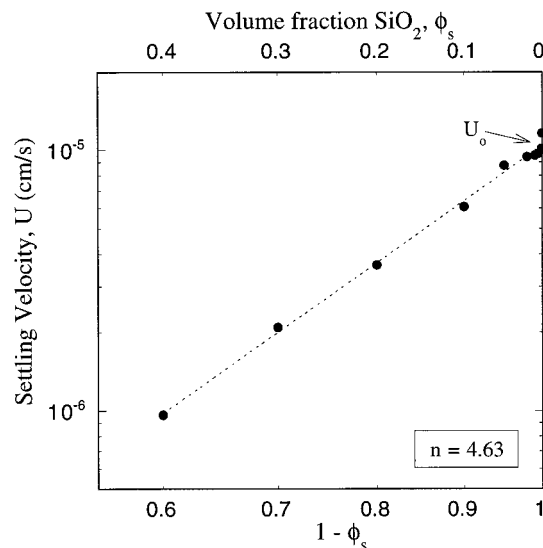


**Fig. 6.** log-log plot of settling velocity as a function of  $\text{SiO}_2$  volume fraction ( $\phi_s$ ) for aqueous suspensions (0.01M  $\text{NH}_4\text{Cl}$ ). Data are fit using Richardson-Zaki form,  $U = U_0(1 - \phi_s)^n$ , where  $n = 4.63$  and  $U_0 = 1.0419 \times 10^{-5}$  cm/s.

therefore higher than would be observed in the absence of gravity-driven effects. When  $\tau_{\text{agg}}/\tau_{\text{sed}} < 1$ , suspensions gel quickly and then settle collectively provided the particle network cannot support its own mass (i.e.,  $\int_0^H \Delta\rho g \phi(z) dz > P_y(\phi)$ , where  $\Delta\rho$  is the density difference between the solid and solution phases,  $g$  is the gravitational constant,  $\phi(z)$  is the volume fraction at a given height,  $z$ ,  $P_y(\phi)$  is the compressive yield stress of the particle network of volume fraction,  $\phi$ , and  $H$  is the suspension height). The upper critical volume fraction,  $\phi_c$ , simply denotes the case where  $\int_0^H \Delta\rho g \phi(z) dz \leq P_y(\phi_s)$ , i.e., when the as-formed gel network can support its own mass.<sup>13</sup>

Flocculated suspensions displayed dramatic variations in settling velocity when  $\phi_s < \phi_c$ , as shown in the inset plot in Fig. 5(b). Similar features have been identified in related work by Allain *et al.*<sup>16</sup> One can define an initial settling velocity,  $U_{\text{initial}}$ , from the linear dependence of the suspension height on time observed at the early stage of this process. The dependence of  $U_{\text{initial}}$  on salt concentration is shown in Fig. 7 for dilute  $\text{SiO}_2$  suspensions ( $\phi_s = 0.01$ , where  $\phi_s < \phi_g$ ). For comparison, the settling velocities of dispersed suspensions are also plotted in Fig. 7. Note, dilute

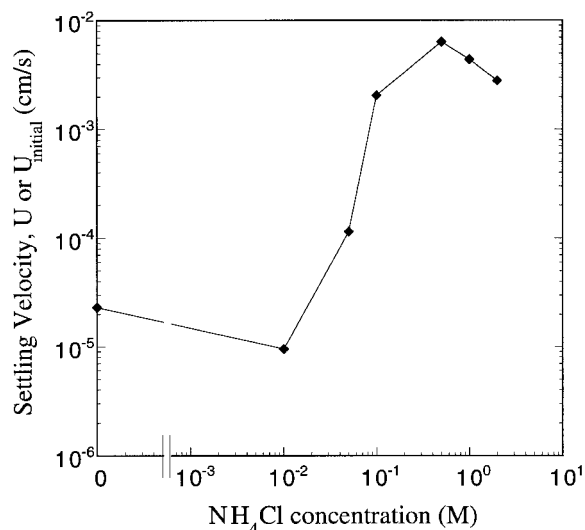


**Fig. 7.** log-log plot of settling velocity as a function of  $\text{NH}_4\text{Cl}$  concentration for aqueous  $\text{SiO}_2$  suspensions ( $\phi_s = 0.01$ ).

systems were chosen to avoid complicating factors arising from gel formation. In such systems, the settling velocity was observed to increase by more than 2 orders of magnitude as the salt concentration increased from 0.07M to 0.10M  $\text{NH}_4\text{Cl}$ . This sudden rise in settling velocity is a hallmark of the transition in suspension stability from a dispersed state  $\rightarrow$  flocculated state, and reflects an increase in the characteristic flow unit (or cluster) size. As expected, given the flow behavior and direct observations of particle clustering, a maximum settling velocity was observed for aqueous suspensions at a salt concentration of roughly 0.5M  $\text{NH}_4\text{Cl}$ .

The final sediment volume fraction,  $\Phi_{\text{sed}}$ , was determined by comparing the equilibrium sediment height,  $H_{\text{sed}}$ , to the initial suspension height,  $H_0$ , and initial  $\text{SiO}_2$  volume fraction,  $\phi_s$ , using the following expression:

$$\Phi_{\text{sed}} = (H_0/H_{\text{sed}})\phi_s \quad (3)$$

This value,  $\Phi_{\text{sed}}$ , is plotted as a function of  $\phi_s$  in Fig. 8 for two representative cases: (1) a dispersed system (0.01M  $\text{NH}_4\text{Cl}$ ) and (2) a weakly flocculated system (0.50M  $\text{NH}_4\text{Cl}$ ). The solid line is shown in Fig. 8 corresponds to the expected behavior in the absence of gravity-driven consolidation. For the dispersed suspensions,  $\Phi_{\text{sed}}$  increased dramatically at low initial  $\text{SiO}_2$  volume fractions ( $\phi_s < 0.1$ ) and then exhibited a slow rise to  $\phi_m$ , where  $\phi_m$  ( $\sim 0.6$ – $0.64$ ) is the maximum solids volume fraction above which flow ceases. For the flocculated suspensions,  $\Phi_{\text{sed}}$  essentially corresponded to the plateau value,  $\phi_c \sim 0.23$ , over a broad range of initial  $\text{SiO}_2$  volume fractions ( $\phi_s < \phi_c$ ). Hence, such suspensions undergo gravity-driven consolidation until the sediment volume approaches the upper critical limit of  $\phi_c$ , upon which the as-formed particle network can support itself.

#### IV. Discussion

A striking feature of our work is the observation that aqueous  $\text{SiO}_2$  suspensions exhibited a maximum instability at a finite  $\text{NH}_4\text{Cl}$  concentration, as evidenced by their flow behavior under both shear and gravitational forces. Here, we examine the origin of these results with an aim of understanding how such species alter the various interparticle forces (i.e., van der Waals, electrostatic, and, possibly, structural forces) that govern colloidal stability in such systems. Additionally, we discuss the implications of such observations on colloidal processing of ceramic films and bulk forms.

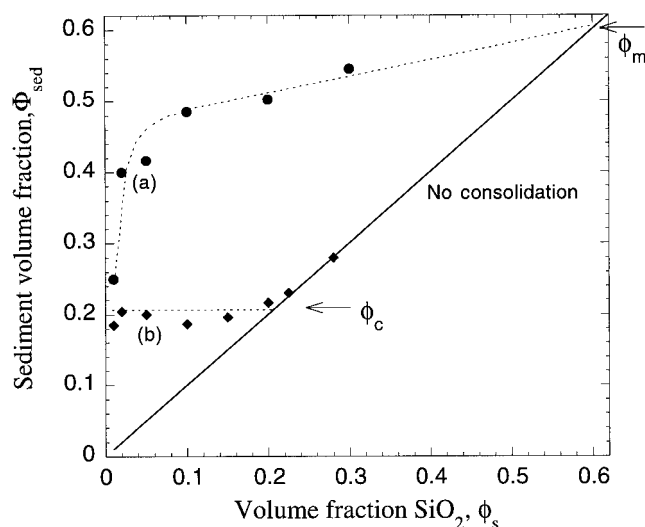


**Fig. 8.** Final sediment volume fraction as a function of initial  $\text{SiO}_2$  volume fraction ( $\phi_s$ ) in suspension for systems with: (a) 0.01M  $\text{NH}_4\text{Cl}$  and (b) 0.50M  $\text{NH}_4\text{Cl}$ . The solid line depicts the behavior expected in the absence of gravity-driven consolidation.

#### (I) Modeling of Colloidal Interactions

The classic DLVO theory has been widely used to model the total interaction potential energy ( $V_{\text{tot}}$ ) of aqueous colloidal suspensions, and is expressed as a sum of attractive potential energy due to long-range van der Waals interaction forces between particles,  $V_{\text{vdw}}$ , and repulsive potential energy arising from electrostatic charges on particle surfaces,  $V_{\text{elect}}$ . For spherical particles of equal size,  $V_{\text{vdw}}$  is given by the Hamaker expression:<sup>19</sup>

$$V_{\text{vdw}} = -\frac{A}{6} \left( \frac{2}{s^2 - 4} + \frac{2}{s^2} + \ln \frac{s^2 - 4}{s^2} \right) \quad (4)$$

where  $s$  is

$$s = \frac{2a + h}{a} \quad (5)$$

$h$  is the minimum separation between the particle surfaces,  $a$  is the particle radius, and  $A$  is the nonretarded Hamaker constant (valid for short separation distances,  $h \leq 5$  nm).<sup>20</sup> A Hamaker constant of  $6 \times 10^{-21}$  J was used in the following analysis. For spherical particles of equal size that approach one another under conditions of constant potential,  $V_{\text{elect}}$  is given by

$$V_{\text{elect}} = 2\pi\epsilon_r\epsilon_0a\Psi_0^2 \ln(1 + \exp(-\kappa h)) \quad (6)$$

when  $\kappa a$  is sufficiently large ( $>10$ ). In contrast, when the double layer around the each particle is extensive ( $\kappa a < 5$ ),  $V_{\text{elect}}$  is given by

$$V_{\text{elect}} = 2\pi\epsilon_r\epsilon_0a\Psi_0^2 \exp(-\kappa h) \quad (7)$$

where  $\epsilon_r$  is the dielectric constant of the solvent,  $\epsilon_0$  is the permittivity of a vacuum,  $\Psi_0$  is the surface potential, and  $1/\kappa$  is the Debye–Hückel screening length.<sup>21</sup> A measured potential of  $-27$  mV was used in the above analysis independent of  $\text{NH}_4\text{Cl}$  concentration.

Using DLVO theory, the calculated potential energy curves for silica–silica interactions in solutions of varying salt concentration are plotted in Fig. 9. As a benchmark, the solid curve depicts the attractive contribution stemming solely from van der Waals interactions. At low  $\text{NH}_4\text{Cl}$  concentrations ( $\leq 0.05$ M), the total interparticle potential energy curve exhibited a strong repulsive barrier exceeding  $30kT$  at short separation distances ( $\sim 1$ – $2$  nm). At moderate  $\text{NH}_4\text{Cl}$  concentrations ( $\sim 0.1$ M), a shallow secondary minimum of a few  $kT$  was observed at separation distances of the order of 5 nm. Hence, this classic theory accurately predicted the

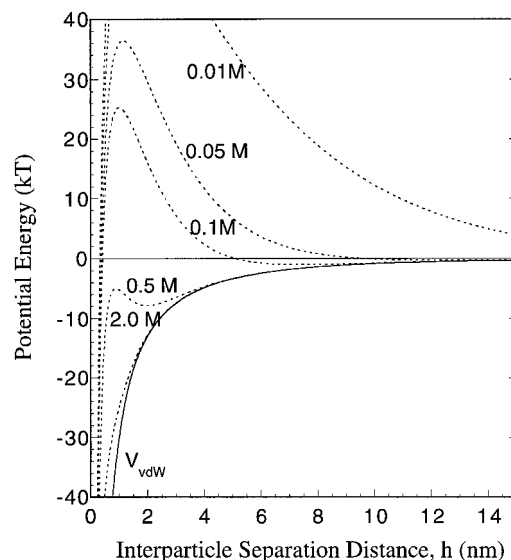


**Fig. 9.** Total interparticle potential energy as a function of separation distance for two  $\text{SiO}_2$  spheres ( $a = 250$  nm) interacting in aqueous solutions of varying  $\text{NH}_4\text{Cl}$  concentration calculated using DLVO theory.

onset of the experimentally observed transition from dispersed to weakly flocculated behavior in this regime ( $\sim 0.07M$   $\text{NH}_4\text{Cl}$ ). However, DLVO theory also predicted that system stability should only decrease with increasing salt additions beyond this point. Thus, it failed to account for the observed restabilization effects at elevated  $\text{NH}_4\text{Cl}$  concentrations ( $\geq 0.5M$ ).

Other contributions to the total interparticle potential energy may give rise to the significant improvements in colloidal stability observed for highly salted, aqueous  $\text{SiO}_2$  suspensions. We have separated such effects into two types; those providing additional terms to  $V_{\text{tot}}$ , such as structural forces, and those directly altering DLVO interaction energies. Short-range structural forces have been measured directly using the surface force apparatus.<sup>22–27</sup> For aqueous solutions, a monotonically decaying repulsive force has been observed which exhibits oscillations with a mean periodicity of 0.25–0.3 nm at separations below 1 nm. These observations were originally attributed by Israelachvili<sup>26</sup> to an extensive association of water molecules bound to hydrated surface groups, and, thus, referred to as a hydration force. More recently, Israelachvili and Wennerstrom<sup>28</sup> have suggested that monotonically repulsive hydration forces may not exist. They propose, in the case of silica, that a small density of charged, inorganic hairs (e.g., silicic acid) extend outward from the solid surface shifting the plane of charge away from the surface plane (i.e., the van der Waals plane). An outward displacement ( $\delta$ ) of the plane of charge by only a few angstroms is all that is needed to recover a short-range, monotonically repulsive force from the summation of  $V_{\text{vdw}}$  and  $V_{\text{elect}}$  contributions alone.<sup>28</sup> Another explanation, which is more broadly applicable, is that this short-range force stems from finite ion size effects. In calculating the electrostatic contribution,  $V_{\text{elect}}$ , using DLVO theory, ions are modeled as point charges and, hence, both the van der Waals plane and the plane of charge are coincident. This assumption, valid at large separation distances, likely breaks down at separations of the order of the ion size, again resulting in a shift between these two planes. Feller and McQuarrie<sup>29</sup> have shown that a short-range, monotonically repulsive force is predicted when such effects are taken into consideration. Alternatively, Prieve and Russell<sup>30</sup> have shown that the Hamaker constant is reduced by a screening factor in highly salted, aqueous solutions, thereby diminishing the strength of the long-range van der Waals interactions. Finally, specific adsorption interactions between ammonium ions and silica may also alter the Hamaker constant. It is plausible that any one or more of the aforementioned contributions could lead to the interesting phenomena we have observed in this work. Clearly, accurate modeling of colloidal interactions in the high-salt regime hinges on developing a better understanding of these complicating factors.

## (2) Implications on Ceramics Processing

Colloidal processing of ceramics derived from weakly flocculated suspensions has received increasing attention. This approach has several advantages including reversible aggregation, minimization of mass-driven segregation (when  $\phi > \phi_g$ ) and sedimentation ( $\phi > \phi_c$ ) as well as good consolidation behavior under externally applied pressure gradients (e.g., as experienced in pressure filtration, osmotic consolidation, or centrifugal casting). Some of these advantages may be particularly useful when processing complex ceramic suspensions, such as single-phase systems with tailored particle size distributions or multiphase systems of varying density or particle size/shape. Their aggregating nature, however, requires that defects arising from cluster formation be minimized either by limiting cluster growth or by tailoring the lubricity of interparticle interactions such that cluster breakdown is easily facilitated under the application of an external force during consolidation.

We have shown that the primary cluster size is influenced strongly by  $\text{NH}_4\text{Cl}$  concentration and initial solids loading in aggregating systems. In the dilute limit,  $\phi_s \rightarrow 0$ , the primary cluster size increased significantly with increasing salt concentrations up to the critical value of  $0.5M$   $\text{NH}_4\text{Cl}$  (see Fig. 7). This trend reflects the increased driving force for aggregation that promotes

cluster growth, as predicted by DLVO theory. In the concentrated limit,  $\phi_s \rightarrow \phi_m$ , a gel network formed via aggregation of primary clusters, whose size decreased with increasing  $\phi_s$ . With these ideas in mind, emerging processing routes rely on transforming dense dispersions into weakly flocculated ones by altering their salt content<sup>4,5</sup> or adjusting pH *in situ* via an enzyme-catalyzed decomposition process.<sup>31</sup> In either approach, the aim is to create aggregating systems with tailored attractive interparticle interactions that yield consolidated bodies with high green densities and minimal density gradients. Recently, Guo and Lewis<sup>32</sup> have shown that severe microstructural inhomogeneities arise during drying of colloidal silica films which contain high  $\text{NH}_4\text{Cl}$  concentrations. As drying proceeds, the salt concentration at the film surface becomes enriched due to the coupling between capillary-driven fluid flow and evaporative processes. Therefore, use of responsive, adsorbed species whose interaction strength can be tailored via changes in solvent quality, temperature, and/or pressure may be a better approach.

## V. Conclusions

We have studied the influence of  $\text{NH}_4\text{Cl}$  concentration on the rheological properties and sedimentation behavior of aqueous silica ( $\text{SiO}_2$ ) suspensions of varying solids volume fraction ( $\phi_s$ ). For the first time, we have shown that there is a critical salt concentration that leads to maximum instability, as evidenced by their flow properties under both shear and gravitational forces. The origin of this unusual observation is not well understood, but likely stems from how salt species alter the various interparticle forces (i.e., van der Waals, electrostatic, and, possibly, structural forces) that govern colloidal stability in such systems. While DLVO theory successfully predicted the observed behavior at salt concentrations below this critical value, it failed to account for modest restabilization effects found at elevated salt concentrations. To achieve the desired interparticle lubricity in weakly attractive systems, one must clearly understand how such species influence such interactions or explore alternate approaches such as use of response, adsorbed species.

## References

- J. W. Goodwin, R. W. Hughes, S. J. Partridge, and C. F. Zukoski, "The Elasticity of Weakly Flocculated Suspensions," *J. Chem. Phys.*, **85**, 559 (1986).
- R. Buscall, I. J. McGown, and C. A. Mumme-Young, "Rheology of Weakly Interacting Colloidal Particles at High Concentration," *Faraday Discuss. Chem. Soc.*, **90**, 115 (1990).
- A. L. Ogden and J. A. Lewis, "Effect of Nonadsorbed Polymer on the Stability of Weakly Flocculated Suspensions," *Langmuir*, **12** [14] 3413–24 (1996).
- B. V. Velamakanni, J. C. Chang, F. F. Lange, and D. S. Pearson, "New Method for Efficient Colloidal Particle Packing via Modulation of Repulsive Lubricating Hydration Forces," *Langmuir*, **6** [7] 1323–25 (1990).
- M. Colic, G. V. Franks, M. L. Fisher, and F. F. Lange, "Effect of Counterion Size on Short Range Repulsive Forces at High Ionic Strengths," *Langmuir*, **13** [12] 3129–35 (1997).
- L. Bergstrom, C. H. Schilling, and I. A. Aksay, "Consolidation Behavior of Flocculated Alumina Suspensions," *J. Am. Ceram. Soc.*, **75** [12] 3305–14 (1992).
- A. Einstein, "A New Determination of Molecular Dimensions," *Ann. Phys.*, **19**, 289–306 (1906); Corrections, *ibid.*, **34**, 591–92 (1911).
- I. M. Krieger and T. J. Dougherty, "A Mechanism for Non-Newtonian Flow in Suspensions of Rigid Spheres," *Trans. Soc. Rheol.*, **3**, 137–52 (1959).
- G. K. Batchelor, "The Effect of Brownian Motion on the Bulk Stress in a Suspension of Spherical Particles," *J. Fluid Mech.*, **83**, 97–117 (1977).
- G. K. Batchelor, "Sedimentation in a Dilute Dispersion of Spheres," *J. Fluid Mech.*, **52** [2] 245–68 (1972).
- M. E. Fagan and C. F. Zukoski, "The Rheology of Charge Stabilized Silica Suspensions," *J. Rheol.*, **41** [2] 373–97 (1997).
- T. Okubo, "Sedimentation Velocity of Colloidal Spheres in Deionized Suspension," *J. Phys. Chem.*, **98**, 1472–74 (1994).
- R. Buscall, "The Sedimentation of Concentrated Colloidal Suspensions," *Colloids Surf.*, **43**, 33–53 (1990).
- A. P. Philipse, B. C. Bonekamp, and H. J. Veringa, "Colloidal Filtration and (Simultaneous) Sedimentation of Alumina and Silica Suspensions: Influence of Aggregates," *J. Am. Ceram. Soc.*, **73** [9] 2720–27 (1990).
- M. Carpineti, F. Ferri, M. Giglio, E. Paganini, and U. Perini, "Salt-Induced Fast Aggregation of Polystyrene Latex," *Phys. Rev. A*, **42** [12] 7347–54 (1990).
- C. Allain, M. Cloitre, and M. Wafar, "Aggregation and Sedimentation in Colloidal Suspensions," *Phys. Rev. Lett.*, **74** [8] 1478–81 (1995).
- J. L. McCall and W. M. Mueller (Eds.), *Microstructural Analysis: Tools and Techniques*. Plenum Press, New York, 1973.

<sup>18</sup>J. F. Richardson and W. N. Zaki, "The Sedimentation of a Suspension of Uniform Spheres under Conditions of Viscous Flow," *Chem. Eng. Sci.*, **8**, 65–78 (1954).

<sup>19</sup>J. N. Israelachvili, *Intermolecular and Surface Forces*. Academic Press, New York, 1992.

<sup>20</sup>J. Mahanty and B. W. Ninham, *Dispersion Forces*. Academic Press, New York, 1976.

<sup>21</sup>R. J. Hunter, *Foundations of Colloid Science*, Vols. 1 and 2. Oxford University Press, Oxford, U.K., 1987 and 1989.

<sup>22</sup>J. N. Israelachvili and G. E. Adams, "Measurement of Forces between Two Mica Surfaces in Aqueous Electrolyte Solutions in the Range of 0–100 nm," *J. Chem. Soc., Faraday Trans. 1*, 975–1001 (1978).

<sup>23</sup>R. M. Pashley and J. N. Israelachvili, "DLVO and Hydration Forces between Mica Surfaces and  $Mg^{2+}$ ,  $Ca^{2+}$ , Sr, and Ba Chloride Solutions," *J. Colloid Interface Sci.*, **97**, 446–55 (1984).

<sup>24</sup>R. G. Horn and J. N. Israelachvili, "Direct Measurement of Structural Forces between Two Surfaces in a Nonpolar Liquid," *J. Chem. Phys.*, **75** [3] 1400–11 (1981).

<sup>25</sup>H. K. Christenson, "Interactions between Hydrocarbon Surfaces in a Nonpolar Liquid: Effect of Surface Properties on Solvation Forces," *J. Phys. Chem.*, **90**, 4–6 (1986).

<sup>26</sup>J. Israelachvili, "Solvation Forces and Liquid Structure, As Probed by Direct Force Measurements," *Acc. Chem. Res.*, **20**, 415–21 (1987).

<sup>27</sup>R. G. Horn, "Surface Forces and Their Action in Ceramic Materials," *J. Am. Ceram. Soc.*, **73** [5] 1117–35 (1990).

<sup>28</sup>J. Israelachvili and H. Wennerstrom, "Role of Hydration and Water Structure in Biological and Colloidal Interactions," *Nature (London)*, **379**, 219–25 (1996).

<sup>29</sup>S. E. Feller and D. A. McQuarrie, "Ionic Size Effects on the Force between Planar Electrical Double Layers," *J. Phys. Chem.*, **97**, 12083–86 (1993).

<sup>30</sup>D. C. Prieve and W. B. Russell, "Simplified Predictions of Hamaker Constants from Lifshitz Theory," *J. Colloid Interface Sci.*, **125** [1] 1–13 (1988).

<sup>31</sup>T. J. Graule, W. Si, F. H. Baader, and L. J. Gauckler, "Direct Coagulation Casting (DCC): Fundamentals of a New Forming Process for Ceramics"; pp. 457 in *Ceramic Transactions*, Vol. 51, *Ceramic Processing Science and Technology*. Edited by H. Hausner, G. L. Messing, and S. Hirano. American Ceramic Society, Westerville, OH, 1995.

<sup>32</sup>J. J. Guo and J. A. Lewis, "Aggregation Effects on the Compressive Flow Properties and Drying Behavior of Colloidal Silica Suspensions," *J. Am. Ceram. Soc.*, **82** [9] 2345–58 (1999). □